



Renal bleeding: imaging and interventions in patients with tumors

- Emad D. Singer¹
- Niloofar Karbasian²
- Douglas S. Katz³
- Vincenzo K. Wong¹
- Mohamed E. Abdelsalam¹
- Nir Stanietzky¹
- Trinh T. Nguyen⁴
- Anuradha S. Shenoy-Bhangle⁵
- Mohamed Badawy⁶
- Margarita V. Revzin⁷
- Mostafa A. Shehata¹
- Mohamed Eltaher¹
- Khaled M. Elsayer¹
- Brinda Rao Korivi¹

¹The University of Texas MD Anderson Cancer Center, Department of Abdominal Radiology, Texas, USA

²The University of Texas Health Sciences Center, Department of Diagnostic and Interventional Radiology, Texas, USA

³New York University, Long Island School of Medicine, Department of Radiology, New York, USA

⁴Billings Clinic Hospital, Department of Diagnostic Radiology, Montana, USA

⁵Harvard Medical School, Massachusetts General Hospital, Department of Radiology, Massachusetts, USA

⁶Wayne State University, Diagnostic Radiology Department, Michigan, USA

⁷Yale University School of Medicine, Department of Radiology, Connecticut, USA

Corresponding author: Khaled M. Elsayer

E-mail: kmelsayer@mdanderson.org

Received 25 April 2024; revision requested 12 May 2024; accepted 21 May 2024.



Epub: 14.06.2024

Publication date: xx.xx.2024

DOI: 10.4274/dir.2024.242822

ABSTRACT

In patients with cancer, spontaneous renal bleeding can stem from a range of underlying factors, necessitating precise diagnostic tools for effective patient management. Benign and malignant renal tumors are among the primary culprits, with angiomyolipomas and renal cell carcinomas being the most common among them. Vascular anomalies, infections, ureteral obstructions, and coagulation disorders can also contribute to renal-related bleeding. Cross-sectional imaging techniques, particularly ultrasound and computed tomography (CT), play pivotal roles in the initial detection of renal bleeding. Magnetic resonance imaging and CT are preferred for follow-up evaluations and aid in detecting underlying enhancing masses. IV contrast-enhanced ultrasound can provide additional information for active bleeding detection and differentiation. This review article explores specific disorders associated with or resembling spontaneous acute renal bleeding in patients with renal tumors; it focuses on the significance of advanced imaging techniques in accurately identifying and characterizing renal bleeding in these individuals. It also provides insights into the clinical presentations, imaging findings, and treatment options for various causes of renal bleeding, aiming to enhance the understanding, diagnosis, and management of the issue.

KEYWORDS

Renal bleeding, renal cell carcinoma, angiomyolipoma, diagnosis, imaging, interventions

Bleeding can be a cause of substantial morbidity in patients with cancer; approximately 10% of individuals diagnosed with cancer experience bleeding episodes.^{1,2} Furthermore, high bleeding rates are frequently observed in patients with advanced-stage cancer and those undergoing anticoagulant therapy. These factors underscore the need for vigilant monitoring and tailored management approaches to address the risk of bleeding in this patient population.²

A diverse range of conditions can lead to spontaneous, non-traumatic, and acute renal bleeding in patients with benign and malignant tumors, highlighting the need for precise diagnostic tools to optimize patient management.³ The primary causes of spontaneous renal bleeding include benign and malignant kidney tumors, with angiomyolipomas (AMLs) and renal cell carcinomas (RCCs) being the most common among them.³⁻⁵ In addition to primary renal tumors, vascular abnormalities affecting the kidneys, infections, ureteral obstructions, and coagulation disorders can also contribute to renal-related bleeding in patients with cancer. Additionally, certain neoplastic conditions can closely mimic renal bleeding.³⁻⁵ Cross-sectional imaging techniques, including computed tomography (CT), magnetic resonance imaging (MRI), and ultrasound, are indispensable in evaluating patients with renal bleeding. They enable the detection of renal bleeding and the identification of its underlying causes.⁶⁻⁸ Interventional radiologists play a vital role in managing patients with active and substantial bleeding.⁹

This paper explores specific disorders associated with or resembling spontaneous acute renal bleeding in patients with cancer; it focuses on the crucial role of advanced imaging techniques in accurately identifying and characterizing renal bleeding in these individuals.³ It also provides insights into the clinical presentations, imaging findings, and treatment options for various causes of renal bleeding, aiming to enhance the understanding, diagnosis, and management of the issue.

Clinical presentations of renal bleeding in patients with cancer

Patients with cancer and renal bleeding vary widely in their clinical presentations; some may be asymptomatic, and others may have potentially life-threatening symptoms. Symptoms may include flank pain, macroscopic hematuria, and a palpable abdominal mass. Flank pain can vary in intensity and nature due to the progressive enlargement of a hematoma due to ongoing extravasation. Potentially severe complications include hemorrhagic shock and acute kidney injury, manifesting as tachycardia, hypotension, pallor, altered mental status, and decreased urine output.¹⁰⁻¹⁴

In patients with spontaneous renal bleeding, extrarenal accumulations of fluid can lead to extrinsic compression of the kidney. This compression, termed Page kidney, may elicit systemic hypertension.¹⁵

The role of imaging in renal bleeding detection and follow-up

Ultrasound and CT are the main imaging modalities used for the initial detection of renal bleeding.² Moreover, CT and MRI are the preferred imaging modalities for the follow-up of patients with renal bleeding. Unenhanced CT is employed to confirm that renal bleeding has resolved. Pre- and post-contrast CT and MRI facilitate the detection of an underlying enhancing mass, which is often present in many patients.³ MRI is an excellent modality for renal bleeding follow-up because of its high contrast resolution and ability to assist in tissue characterization without ionizing radiation.³ However, it has limitations: longer scanning times and limited accessibility compared with those of oth-

er modalities and higher prices compared with CT. Follow-up imaging at 2–3 month intervals to document the resolution of the hemorrhage is of utmost importance in patients with bleeding whose underlying cause remains unclear.³ If subsequent scans do not reveal the presence of an underlying mass, no additional measures are required, assuming the hemorrhage continues to diminish in size and a thorough assessment of the underlying renal structure is conducted.³ Table 1 summarizes the appearance of renal bleeding on various imaging modalities according to the phase of the bleeding.^{5,16-19}

Ultrasound

Ultrasound is a valuable imaging modality for assessing hematomas with distinct characteristics observed at different stages of development.¹⁷ An acute hematoma initially appears solid and hyperechoic, or heterogeneous on gray-scale ultrasound, and avascular on color Doppler imaging (Figure 1).¹⁷ As the hematoma progresses, it changes its echotexture and becomes more heterogeneous. Occasionally, it has a central region of decreased echogenicity or a cystic-like appearance. In the chronic phase, peripheral calcifications may develop within the hematoma.¹⁷

Intravenous (IV) contrast-enhanced ultrasound can potentially depict active renal bleeding.¹⁸ Moreover, when a substantial renal mass or a conspicuous vascular anomaly is absent, ultrasonography might not suffice to ascertain the underlying cause of bleeding in most patients with spontaneous renal bleeding. The use of contrast-enhanced ultrasound provides supplementary information beyond that which conventional ultrasound methodologies can offer.^{18,20-26}

Computed tomography

On non-contrast CT, acute bleeding has an attenuation value of 30–45 Hounsfield units (HU),^{5,16} and this value increases to 60–80 HU after several hours, depending on the concentration of hemoglobin.^{5,16} In the subacute phase (several days to several weeks), the attenuation of the bleeding decreases as the blood clot is resorbed, resulting in the formation of a seroma with an attenuation value of approximately 30 HU or less.^{5,16} Calcification may be visible in cases of chronic hematomas, defined as those present for more than 1–2 months. If an IV contrast-enhanced CT is performed during acute bleeding, active contrast extravasation from the underlying bleeding vessel may be localized in the arterial phase of the CT.^{5,16} CT can also help differentiate between extravasations

Table 1. The appearance of renal bleeding by imaging modality and phase

Imaging modality	Appearance in the acute phase	Appearance in the subacute and chronic phases
Ultrasound	Solid and echogenic appearance	Appearance is stable or reduced in size
	Multi-lamellated, whorled appearance	Hypoechoic fluid collections due to liquefaction
	Anechoic cystic areas	Formation of retractile clots/angular margins
	Surrounding soft-tissue edema	An increase in size may simulate a soft-tissue tumor Well-defined margin, distinct capsule Hypoechoic or anechoic seroma with posterior acoustic enhancement
Non-contrast CT	Normally, the attenuation value of the bleeding would be 30–45 HU, similar to the blood pool's attenuation	Bleeding attenuation decreases due to clot lysis and progressive seroma formation, measuring approx. 30 HU or less
	Bleeding typically measures 60–80 HU during the hyperacute phase, which lasts a few hours	Chronic hematomas can calcify
MRI	Hyperacute blood: T1 isointense, T2 hypointense	Early subacute (2–7 days): T1 hyperintense, T2 hypointense
	Acute blood: T1 hypointense/isointense, T2 hypointense	Late subacute (7–14 days): T1 hyperintense, T2 hyperintense
		Chronic: peripherally low T1 and T2 signals, central T1 isointense and T2 hyperintense

CT, computed tomography; MRI, magnetic resonance imaging; HU, Hounsfield units.

Main points

- There are numerous causes of spontaneous renal bleeding; tumors, both benign and malignant, vascular malformations, infection, and coagulopathy are common etiologies.
- Utilizing the most appropriate diagnostic tools to determine the cause is critical, and ultrasound and computed tomography (CT) are most often used in the acute setting, whereas CT and magnetic resonance imaging play an important role in follow-up.
- Catheter angiography plays an important role in the management of renal bleeding.
- The many causes of bleeding are discussed with examples; pitfalls, including mimickers of bleeding, are also presented.

and pseudoaneurysms. Active extravasation manifests as an ill-defined area of extraluminal contrast. During the arterial phase, it appears isointense to the blood pool. Subsequently, it persists during the portal venous phase and typically enlarges progressively in the delayed phase.²⁷ In contrast, a pseudoaneurysm is characterized by a well-defined, rounded mass with an internal enhancement that matches the pattern observed in the aorta on corticomedullary phase images.²⁸

Magnetic resonance imaging

The appearance of bleeding on MRI changes depending on the chronicity of the bleeding and the breakdown of the hemoglobin over time (Figure 2).¹⁹ In the early stage, compared with the surrounding tissues, the bleeding appears isointense on T1-weighted images and isointense to hyperintense on T2-weighted images. This is attributed to the diamagnetic effect of intra-

cellular oxyhemoglobin.¹⁹ In the acute phase, hemoglobin breaks down into intracellular deoxyhemoglobin, causing a decrease in the signal intensity on both T1- and T2-weighted images. In the early subacute phase (4–7 days), hemoglobin breakdown leads to the formation of intracellular methemoglobin, which has a paramagnetic effect that causes a hyperintense signal on T1 images and a hypointense signal on T2 images.¹⁹ In the late subacute phase (1–4 weeks), the continued breakdown of hemoglobin forms extracellular methemoglobin, contributing to a hyperintense signal on both T1 and T2 images. During the chronic stage, the bleeding demonstrates a peripheral area of low-signal intensity on both T1- and T2-weighted images, which can be attributed to the accumulation of intracellular hemosiderin, and the central region displays T2 hyperintensity and T1 isointensity.¹⁹

A hemorrhage can be detected and differentiated from the surrounding tissues using susceptibility-weighted imaging (SWI), a sequence combining the magnitude and phase data of MRI. It is sensitive to the detection of blood products, including microhemorrhages.^{29–32}

Owing to its sensitivity and ability to depict changes in hemoglobin types as a hematoma ages, SWI can be very useful in identifying hemorrhages.³³ Its sensitivity and accuracy can surpass those of conventional imaging methods routinely used to detect bleeding; it can depict and characterize hemorrhage in clear cell RCCs, regardless of the tumor grade or bleeding pattern.³⁴ However, SWI images can be affected by air-caused susceptibility artifacts within the gastrointestinal tract, leading to imaging patterns that resemble bleeding and potentially complicating the interpretation of images.³⁴

Catheter angiography

Superselective renovascular catheterization and embolization play crucial roles in the diagnosis and treatment of renal bleeding and, potentially, the avoidance of radical surgery (Figure 3). Interventional radiology management strategies, particularly the coiling or embolization of the bleeding source, are used for treatment. Renal arteries are terminal vessels that lack substantial intrarenal collateral circulation. Hypervascular renal tumors, particularly RCCs, make use of collateral circulation from outside the kidneys. Hence, the preferred embolic agents are those that can block small vessels, including N-butyl cyanoacrylate glue, ethanol, polyvinyl alcohol, or embospheres, as well as agents capable of occluding larger vessels (e.g., coils).³⁵ The potential complications of endovascular treat-

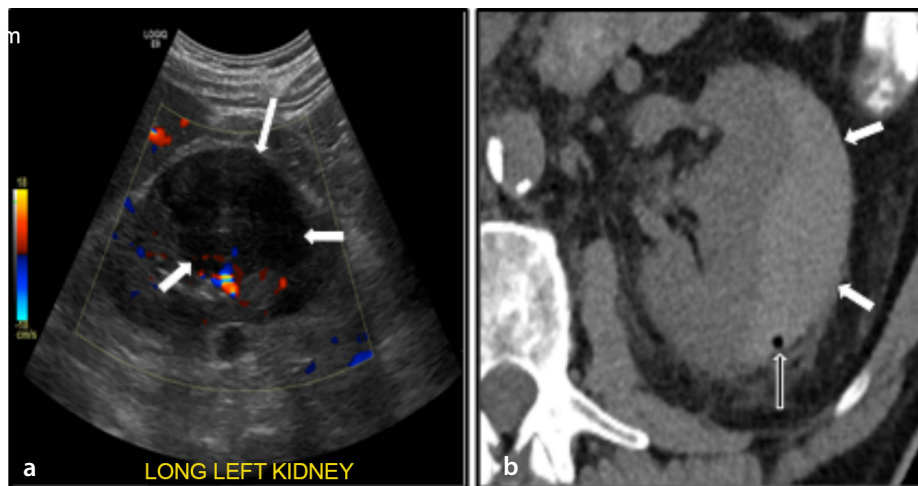


Figure 1. A lentiform, mass-like area along the lateral margin of the left kidney is seen on color Doppler ultrasound (a) and axial non-contrast CT (b), consistent with an acute subcapsular hematoma (white arrows). A tiny focus of gas along the posterior margin is likely iatrogenic (black arrow). CT, computed tomography.

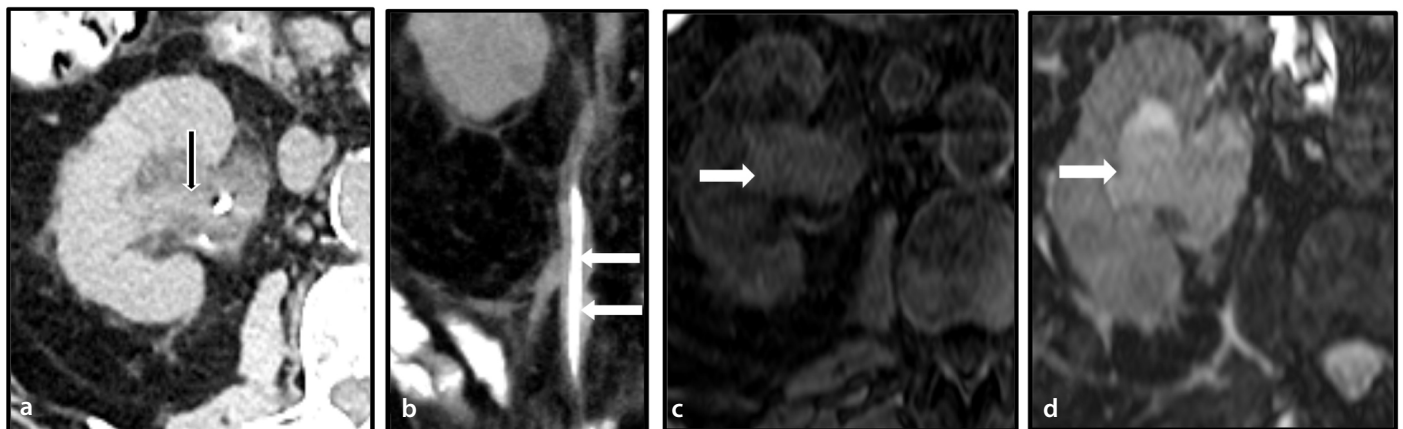


Figure 2. Axial (a) and coronal (b) contrast-enhanced CT status scans obtained after the placement of a right nephroureteral stent in a patient with urothelial carcinoma (white arrows). The high-attenuation hemorrhage within the renal pelvis is consistent with hemorrhage (black arrow). (c, d) Non-contrast T1 (c) and T2 (d) MRI images of the right kidney demonstrate layering of late subacute blood products (T1 hyperintense, T2 hyperintense) (white arrows). CT, computed tomography; MRI, magnetic resonance imaging.

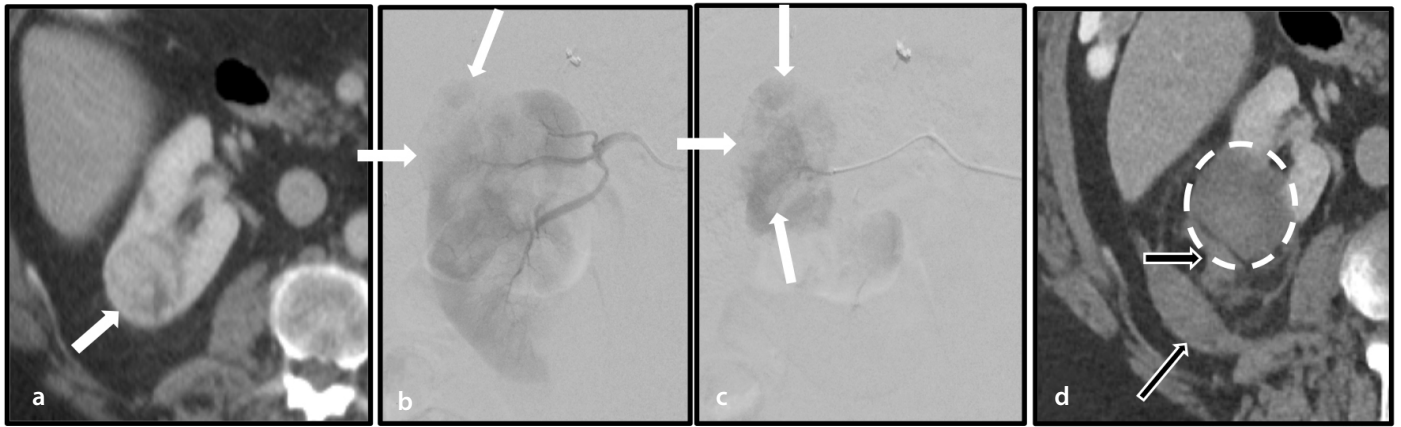


Figure 3. (a) A right upper pole renal cell carcinoma (white arrows) demonstrates abnormal tortuous intra-tumoral vessels on angiography (b) during pre-ablation renal artery embolization (b, c). Post-ablation contrast-enhanced CT (d) demonstrates a hypoattenuating ablation zone without residual enhancement (white circle). A small amount of posterior perirenal hemorrhage is present (black arrows). CT, computed tomography.

ment include infarction, exacerbation of hypertension, unintended embolization (e.g., coil migration to the systemic circulation), and stent graft thrombosis.³⁵

Primary renal neoplasms

Renal cell carcinoma

RCC can cause spontaneous bleeding within the renal parenchyma; it is the most common cause of spontaneous bleeding due to a primary malignant renal neoplasm (Figures 4, 5).^{3,36} Parenchymal bleeding is more frequently observed in the clear cell subtype of RCC, which is the most prevalent subtype.⁸ CT and MRI are useful in diagnosing RCC, but they can pose challenges in identifying the tumor if it is small and obscured by bleeding. In such cases, subtraction imaging may aid in identifying the underlying tumor.³ However, it can cause several problems: misregistration artifacts related to patient motion and a variation in the technical factors on the unenhanced and enhanced sequences.³⁷ An alternative strategy to identify small tumors presenting with bleeding and potentially obscured on the initial scans is to repeat imaging after the hematoma shrinks (6–8 weeks). Table 2 summarizes the differential diagnoses of spontaneous renal bleeding in patients with cancer and includes helpful radiological features for proper differentiation.

For patients presenting with bleeding in association with RCC, a patient's clinical condition dictates the treatment. Hemodynamically stable patients are treated conservatively and monitored closely. However, transcatheter arterial embolization (TAE) may be needed to treat active bleeding or prevent it from increasing by cutting off the tumor's blood supply.⁸ The disease stage must be

Table 2. Differential diagnoses and the main radiological features of renal bleeding in patients with cancer

Diagnosis	Radiological features
Renal cell carcinoma	Heterogeneous, solid renal mass Enhancement with contrast on CT or MRI scans Possible bleeding (high-density areas on non-contrast CT scans, hyperintense areas on T1-weighted MRI scans) Invasion into the renal vein or inferior vena cava in advanced cases
Trauma/ iatrogenic bleeding (e.g., after renal biopsy, nephrostomy placement)	Perirenal hematoma (fluid collection around the kidney) Laceration or contusion of the kidney parenchyma Active extravasation (contrast extravasation on CT scans) Urinoma or urinary leakage (with collecting system injury)
Vascular causes (e.g., polyarteritis nodosa)	Multiple, small, round, wedge-shaped, or irregular hypodense foci on CT scans Enhancement of peripheral rims in the arterial phase Rosary sign or string-of-beads appearance on renal artery due to microaneurysms on angiography
Angiomyolipoma	Well-circumscribed, hyperechoic mass on ultrasound Fat-containing mass with negative HU on CT scans T1 and T2 are hyperintense signals on MRI scans (without fat suppression) Presence of bleeding (high-density areas on non-contrast CT scans and hyperintense areas on T1-weighted MRI, with fat suppression to differentiate between the bleeding and fat content) No specific features for renal bleeding, but bleeding may occur due to infection or obstruction Multiple, bilateral, low-attenuation renal masses on CT scans Homogeneous or heterogeneous enhancement with contrast Bleeding may be present with aggressive subtypes or as a complication

CT, computed tomography; MRI, magnetic resonance imaging; HU, Hounsfield units.

considered when choosing a definitive treatment for RCC. Percutaneous ablation, partial nephrectomy, and radical nephrectomy are alternative therapeutic approaches that can

be employed, depending on the tumor stage and location and the general health of the patient, among other factors.³⁸

Angiomyelipoma

Various studies have shown that the prevalence of renal AMLs as a causative factor for spontaneous renal bleeding ranges from 30% to 35%.³⁶⁻³⁹ Typically affecting the kidneys, AMLs are a condition in which mesenchymal tumors characterized by variable amounts of mature smooth muscle, adipose tissue, and abnormal blood vessels form.⁴⁰ It is assumed that AMLs originate from perivascular epithelioid cells, which are unique cells found close to blood vessels.⁴⁰ Classic triphasic and monotypic epithelioid AMLs are the two primary subtypes of the disease, and these subgroups have distinct biological and imaging properties. Up to 70% of classic AMLs appear sporadically, and 30%–50% are linked to tuberous sclerosis, according to older literature. However, the vast majority of AMLs are now found incidentally on imaging examinations performed for other reasons and are small or relatively small.⁸ Approximately 5% of all renal AMLs are epithelioid and exhibit aggressive behavior that predisposes patients to recurrence, metastasis, and death.⁴¹

There is a risk of spontaneous renal bleeding in patients with renal AMLs, regardless of the origin or histological subtype, and this is particularly true for patients with medium or large-sized AMLs (greater than 4 cm).^{8,42-44} On CT imaging, classic AMLs typically appear as heterogeneous masses characterized by a mixture of macroscopic fat, hypervascular soft-tissue components, and intratumoral aneurysms.⁴⁵ In cases of spontaneous renal bleeding, the CT appearance of AMLs can be altered due to intratumoral and perirenal bleeding. MRI shows high signal intensity on T1-weighted images and signal loss on fat-saturated sequences, indicating the presence of macroscopic fat within the renal AMLs. On imaging, epithelioid AMLs are similar to other solid renal masses because they often lack macroscopic fat and appear as solid, soft-tissue masses. Therefore, they cannot be reliably distinguished from other renal tumors by imaging alone.⁸

Up to 25% of renal AMLs have the potential to rupture spontaneously, leading to perinephric bleeding.⁴¹ The presence of abnormal arteries in AMLs -arteries characterized

by a reduced elastin content- increases their susceptibility to aneurysm development.⁸ The likelihood of rupture, potentially resulting in life-threatening bleeding, increases with the size of tumoral aneurysms.⁴⁶ The frequency of tumor rupture and intratumoral bleeding is substantially influenced by the size of the tumor and the intratumoral aneurysms.⁸ Concerning tumor-related bleeding in AMLs, a larger tumor size (>4 cm) is directly correlated with a larger diameter of intratumoral aneurysms (>5 mm).⁴⁷ CT and/or MRI imaging modalities can depict the presence of the tumor associated with spontaneous renal bleeding produced by ruptured AMLs. However, it is important to note that the imaging appearance of the tumor may be modified due to bleeding.⁸ Furthermore, CT findings can aid in differentiating AMLs from liposarcoma, because the scans of AMLs are more likely to show small dimensions, lack of renal tissue, multiple vessels, aneurysmal dilation, vascular pedicle, bleeding, encapsulated periphery, and fatty lesions.⁴⁸ Kış et al.⁴⁹ have suggested the use of diffusion-weighted imaging and apparent diffusion coefficient (ADC) values for renal

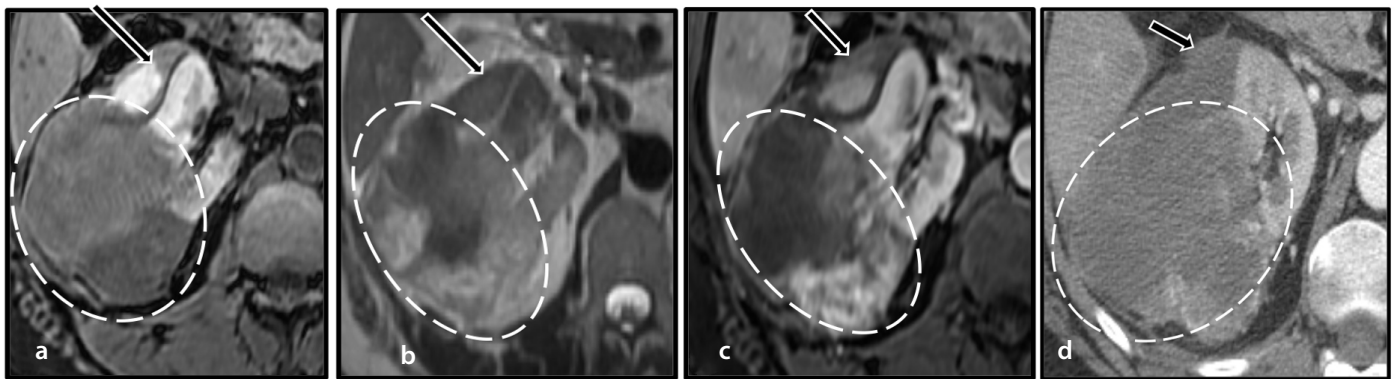


Figure 4. An axial MRI at the level of the right kidney (a-c) demonstrates a heterogeneous mass (white circle) with regions showing a non-enhancing, mildly T1 hyperintense signal, suggesting hemorrhage/necrosis. The findings are consistent with the patient's known renal cell carcinoma. An associated subacute subcapsular hematoma (black arrows) compresses the renal parenchyma. (d) An axial contrast-enhanced CT of the right kidney demonstrates the mass (white circle) and associated subcapsular hematoma (black arrow). MRI, magnetic resonance imaging; CT, computed tomography.

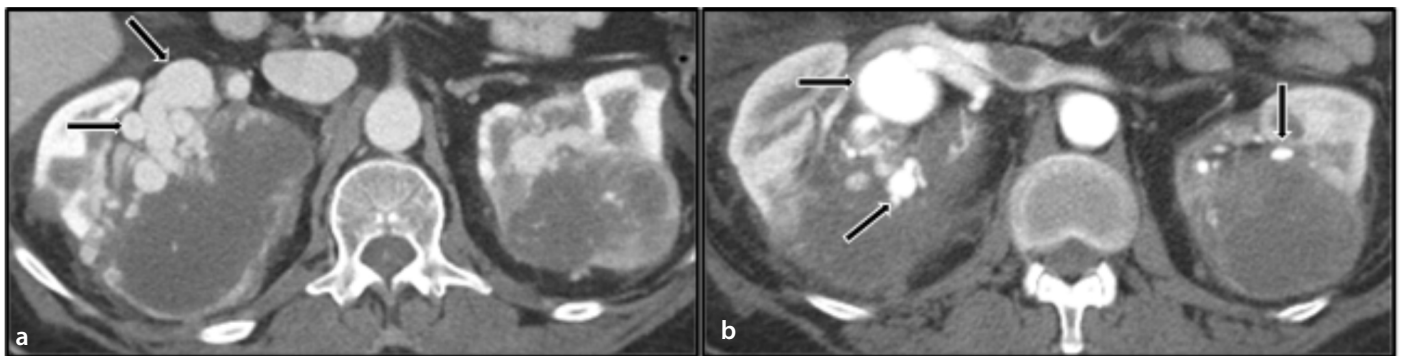


Figure 5. Axial CT images (a, b) demonstrate bilateral renal cell carcinomas with invasion of the renal hila. Multiple bilateral dilated vessels and aneurysms are present in the renal hilar regions (black arrows). Renal cell carcinoma is commonly associated with a variety of vascular anomalies, including renal artery aneurysms and arteriovenous fistulas. CT, computed tomography.

mass classification. They found that benign lesions demonstrate higher ADC values than the adjacent normal renal parenchyma; they also discovered that the ADC of malignant tumors is lower than that of the adjacent parenchyma. In their study, the ADC values were lowest in AMLs and oncocytomas.⁴⁹ Figures 6 and 7 illustrate bleeding secondary to AMLs.

TAE is the primary treatment modality for patients experiencing acute bleeding; it effectively achieves hemostasis in approximately 96% of cases, preventing emergency surgery.⁵⁰ To minimize bleeding events, prophylactic TAE reduces the size and vascularity of large AMLs.⁵¹ Prophylactic, selective TAE shows greater tumor reduction benefits in AMLs with a diameter of less than 7 cm, according to Hongyo et al.⁵² Angiographic observations (e.g., of vascularity and intratumoral aneurysms) allow the classification of AMLs into categories with minimal, moderate, and marked vascularity. Such classifications are valuable guides for determining

the appropriate prophylactic treatment.⁴⁷ In cases in which TAE fails to achieve the desired outcome, nephron-sparing surgery is typically performed. However, when more invasive interventions are warranted (e.g., in patients with a suspected malignancy or uncontrolled bleeding in an emergency scenario), total nephrectomy may be a treatment option for large AMLs.⁵³

Renovascular conditions in patients with cancer

Renal vein thrombosis

Renal vein thrombosis occurs when the primary renal veins or their branches become blocked owing to thrombosis or embolism. In rare instances, it can predispose a patient to spontaneous renal bleeding.⁵⁴ Neoplasms, primarily RCCs, preferentially infiltrate the renal vein, especially when they become large and more locally aggressive, resulting in renal vein thrombosis. In cases in which the tumor is significantly large, it can extend

into the inferior vena cava. Additionally, extrinsic compression resulting from the mass effect of the tumor can produce a prothrombotic milieu without direct vein invasion. In patients with renal vein thrombosis, renal bleeding likely results from renal parenchymal edema and necrosis, potentially leading to renal capsular rupture.^{54,55}

On cross-sectional imaging, a patient with renal vein thrombosis typically presents with an enlarged ipsilateral kidney and edema in the renal sinus and perirenal space.⁵⁶ A complete or partial renal vein thrombosis can be identified by the absence or reduction of renal parenchymal enhancement on nephrographic-phase images. On IV contrast-enhanced CT and MRI, the thrombus in the renal vein appears as a filling defect.⁵⁶ For patients with renal vein thrombosis, the first-line treatment involves medical management with anticoagulation therapy. In select cases, catheter-guided thrombectomy and filter placement in the inferior vena cava are the preferred treatment options.⁵⁴

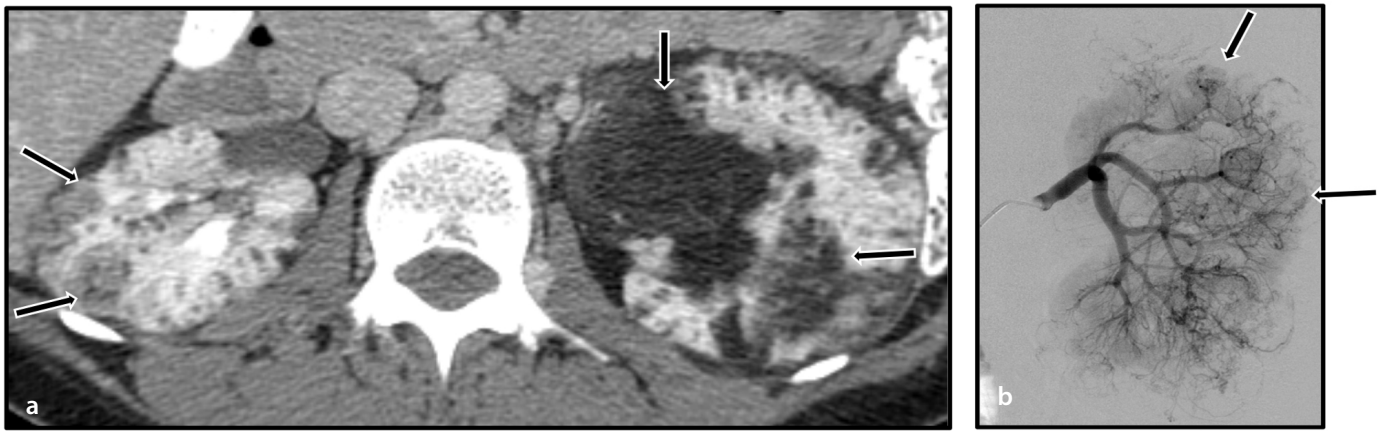


Figure 6. An axial contrast-enhanced CT scan (a) at the level of the kidneys demonstrates innumerable bilateral renal masses with intralesional macroscopic fat, diagnostic of angiomyolipomas (AMLs) (black arrows). Bilateral AMLs, the most common renal neoplasm associated with spontaneous hemorrhage, are seen in 95% of patients with tuberous sclerosis complex. They have the propensity to form pseudoaneurysms and present a higher risk of bleeding if they reach a size of >4 cm. (b) Digital subtraction angiography of the left kidney demonstrates opacification of the renal arteries with multiple tortuous tumor vessels and pseudoaneurysms (black arrows). This pattern is typical of multiple AMLs in the setting of tuberous sclerosis. CT, computed tomography.

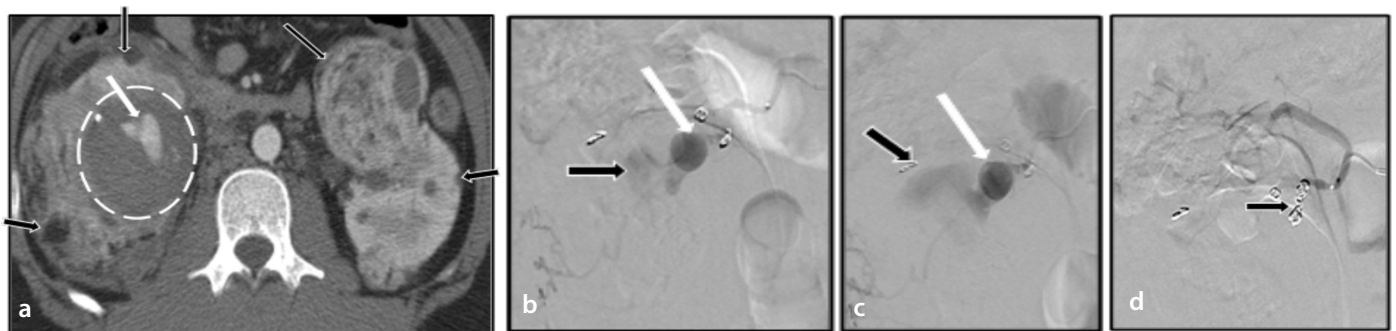


Figure 7. An axial contrast-enhanced CT (a) through the kidneys demonstrates numerous bilateral angiomyolipomas (black arrows). A hematoma is present in the right medial midpole (white circle), with central pseudoaneurysms (white arrow). (b, c) Digital subtraction angiography images of the right kidney demonstrate the pseudoaneurysm (white arrow) with active contrast extravasation (black arrow) into the retroperitoneum, which was subsequently treated with coil embolization (d) (black arrow). CT, computed tomography.

Renal artery abnormalities

Vascular anomalies related to malignant tumors, including renal artery aneurysms, pseudoaneurysms, or renal arteriovenous fistulas (AVFs), are among the main causes of spontaneous perinephric bleeding in patients with cancer.³⁶ Additionally, renal vascular injury may occur in a postprocedural kidney following renal biopsy or nephrostomy tube placement. Pseudoaneurysms demonstrate the classic yin-yang sign on Doppler ultrasound owing to the swirling motion of the blood in the sac. On CT angiography (CTA) and MR angiography (MRA), pseudoaneurysms are seen as outpouchings of the renal arteries that follow the blood pool (Figures 8-10). Renal AVFs appear on ultrasound as areas of aliasing artifacts. In rare cases, a color flash is observed, sometimes referred to as a visible thrill; it is caused by soft-tissue vibrations around the renal AVF that lead to a distinct color mosaic overlying

the adjacent tissue. Spectral analyses of AVFs demonstrate elevated peak systolic velocities, spectral broadening, reduced resistive indexes, and arterialization of the draining veins.² Identifying small renal AVFs might pose challenges during CTA and MRA, but when they are identified using these imaging techniques, they display abnormal arteriovenous connections with early draining venous channels.

Despite its low incidence, the rupture of a renal artery aneurysm or an AVF is associated with substantial mortality. The rupture can be confirmed using arterial-phase CT imaging, which displays active extravasation of contrast material with attenuation similar to that of the blood pool, as noted earlier.³

Although TAE can be used to successfully treat less severe episodes of bleeding, an immediate nephrectomy may be necessary in cases of severe bleeding.⁵⁷ Considering

the dangers of disease development and recurrence, TAE is the preferred therapeutic approach. Employing nephron-sparing interventions is recommended to preserve renal function. For unruptured large renal artery aneurysms greater than 2 cm in diameter, prophylactic embolization may be necessary.^{49,50} Endovascular intervention has emerged as a safe and effective method for managing renal artery aneurysms and may replace surgery as the primary therapeutic approach.⁵⁷⁻⁵⁹ Renal artery aneurysms less than 2 cm in diameter can be closely monitored through follow-up imaging. However, prompt embolization is imperative.^{59,60} Prophylactic TAE is recommended for renal artery aneurysms at high risk of rupture and for symptomatic patients.^{59,60}

Potential mimics of renal bleeding

Lymphoma affecting the kidneys is commonly observed in widespread non-Hodgkin



Figure 8. Axial CT images pre-biopsy (a) and post-biopsy (b) of a right renal mass (black arrows) demonstrate a large amount of perinephric hemorrhage post-biopsy (black arrows). Foci of contrast blush may represent pseudoaneurysms and/or active bleeding (white arrows). (c) An angiogram of the left kidney demonstrates active contrast extravasation in the mid kidney (white arrow). CT, computed tomography.

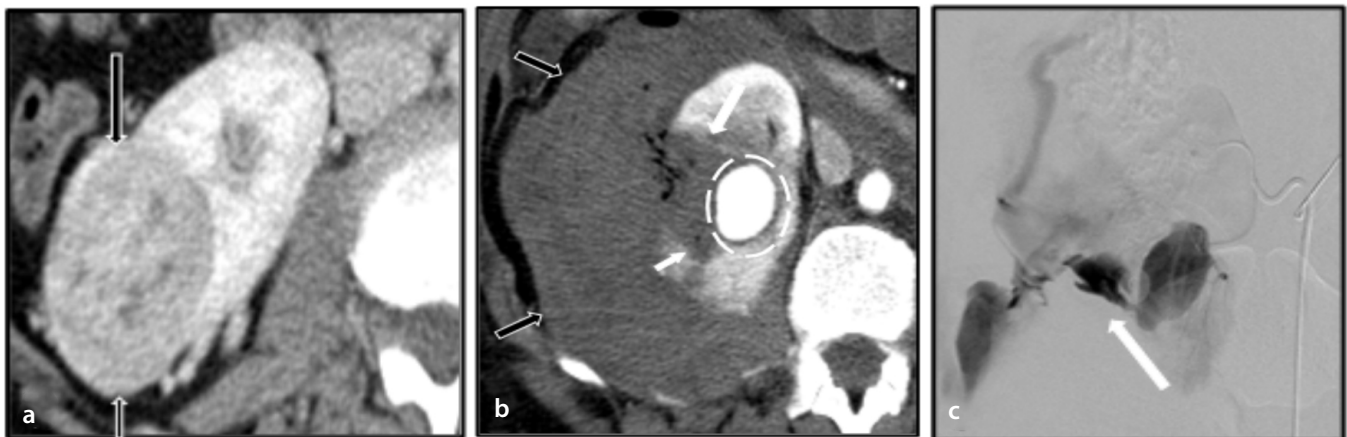


Figure 9. Axial contrast-enhanced CT images pre- (a) and post-biopsy (b) of a right renal mass (black arrows in a) demonstrate the development of a large pseudoaneurysm status post-biopsy (white circle), right renal parenchymal laceration (white arrows in b), and a large perinephric hematoma (black arrows in b). An angiogram (c) demonstrates an active contrast extravasation (white arrow) that was subsequently treated with coil embolization. CT, computed tomography.

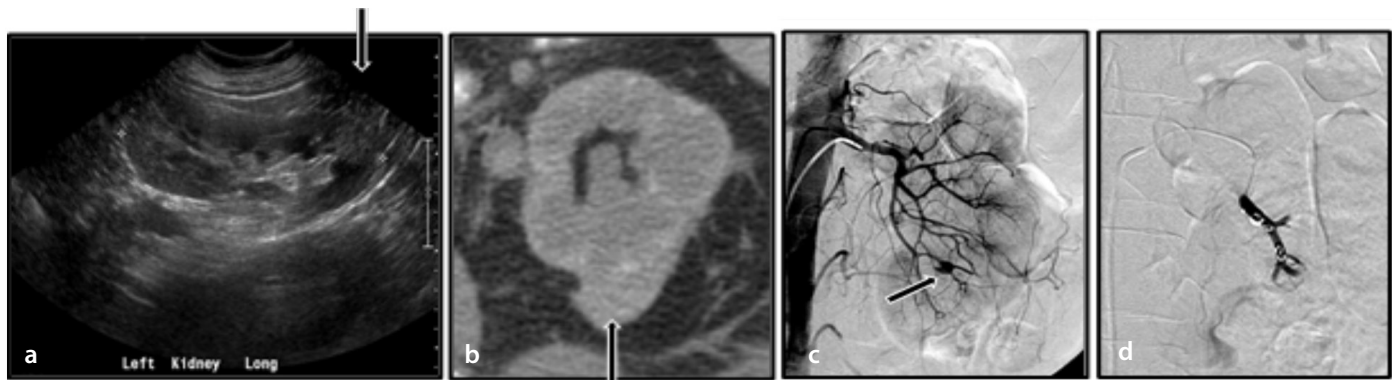


Figure 10. (a) A grayscale ultrasound of the left kidney after a non-targeted renal biopsy demonstrates a hyperechoic mass-like area in the left kidney lower pole (black arrow). (b) An axial non-contrast CT confirms a small subcapsular hematoma (black arrow). (c, d) A digital subtraction angiography of the left kidney demonstrates a small pseudoaneurysm (black arrow in c), which was subsequently embolized (d). CT, computed tomography.



Figure 11. (a) An axial image from a contrast-enhanced CT scan in a 68-year-old man with a biopsy-proven perinephric lymphoma demonstrates a high attenuation mass (58 HU) surrounding the lower pole of the left kidney. This is also seen in the coronal reformatted image (b). The pre-contrast scan (c) at the same level demonstrates that the mass is of lower attenuation (32 HU), and the diffuse enhancement is suggestive of a mass rather than a hemorrhage. CT, computed tomography; HU, Hounsfield units.

lymphoma and is more prevalent in patients with a weakened immune system.^{3,61} The appearance of renal lymphoma on imaging depends on the growth pattern and histology of the tumor.⁶¹ The typical imaging presentation of renal lymphoma consists of multiple parenchymal masses of variable sizes, usually ranging from 1 to 4.5 cm in diameter.⁶¹⁻⁶⁵ This pattern is observed in approximately 50%–60% of cases. Although these masses are often bilateral, they can also be unilateral.⁶¹⁻⁶⁵ On unenhanced CT, these masses exhibit soft-tissue characteristics with slightly higher attenuation than the surrounding renal parenchyma.⁶¹ Calcifications within the tumoral foci are infrequent. It is crucial to employ IV contrast-enhanced CT scanning during the nephrographic phase because many tumoral foci are small and primarily involve the medullary region of the kidneys, resulting in subtle cortical deformity. Lymphomatous deposits exhibit less enhancement than normal renal tissues and appear as relatively homogeneous masses with lower attenuation than the surrounding cortex.⁶¹ Perinephric lymphoma can exhibit various attenuation values on CT and can mimic perirenal hematoma

by encasing the perirenal soft tissue around the blood vessels (Figure 11). It is critical to accurately distinguish fluid, blood products, and inflammation from soft-tissue masses. Homogeneous, relatively mild enhancement is characteristic of perirenal lymphoma, and the perinephric fat may separate the tumor from the kidney. Moreover, lymphoma can be staged using positron emission tomography and CT.^{3,61}

In conclusion, renal bleeding presents a substantial challenge in managing patients with cancer, particularly those with RCC or those undergoing anticoagulant therapy. Diagnostic cross-sectional imaging techniques, including ultrasonography, CT, and MRI, are crucial for identifying and evaluating the etiology of renal bleeding. SWI is useful in detecting and characterizing renal masses associated with renal bleeding, especially microhemorrhages. Therapeutic options range from the observation of stable patients to TAE for active bleeding control. Treatment options for RCC vary depending on the disease stage: ablation, partial nephrectomy, or radical nephrectomy. Prospective studies comparing different treatment modalities

(e.g., TAE, nephron-sparing surgery, and total nephrectomy) in specific patient subgroups provide valuable insights into personalized treatment approaches. Addressing these gaps can enhance the understanding of renal bleeding in patients with cancer, improve evidence-based diagnosis, management, and prevention recommendations, and ultimately enhance patient outcomes and quality of life.

Acknowledgments

We thank Laura L. Russell, scientific editor of Research Medical Library, for editing this article.

Conflict of interest disclosure

The authors declared no conflicts of interest.

References

1. Pereira J, Phan T. Management of bleeding in patients with advanced cancer. *Oncologist*. 2004;9(5):561-570. [CrossRef]
2. Lyman GH, Eckert L, Wang Y, Wang H, Cohen A. Venous thromboembolism risk in patients

- with cancer receiving chemotherapy: a real-world analysis. *Oncologist*. 2013;18(12):1321-1329. [\[CrossRef\]](#)
3. Hammond NA, Lostumbo A, Adam SZ, et al. Imaging of adrenal and renal hemorrhage. *Abdom Imaging*. 2015;40(7):2747-2760. [\[CrossRef\]](#)
 4. Bosniak MA. Spontaneous subcapsular and perirenal hematomas. *Radiology*. 1989;172(3):601-602. [\[CrossRef\]](#)
 5. Furlan A, Fakhran S, Federle MP. Spontaneous abdominal hemorrhage: causes, CT findings, and clinical implications. *AJR Am J Roentgenol*. 2009;193(4):1077-1087. [\[CrossRef\]](#)
 6. Mao Y, De Oliveira IS, Hedgire S, Prapruttam D, Harisinghani M. Aetiology, imaging features, and evolution of spontaneous perirenal haemorrhage. *Clin Radiol*. 2017;72(2):175. [\[CrossRef\]](#)
 7. Diaz JR, Agriantonis DJ, Aguila J, Calleros JE, Ayyappan AP. Spontaneous perirenal hemorrhage: what radiologists need to know. *Emerg Radiol*. 2011;18(4):329-334. [\[CrossRef\]](#)
 8. Katabathina VS, Katre R, Prasad SR, Surabhi VR, Shanbhogue AK, Sunnapwar A. Wunderlich syndrome: cross-sectional imaging review. *J Comput Assist Tomogr*. 2011;35(4):425-433. [\[CrossRef\]](#)
 9. Gong M, Liu Z, Su H, Zhao B, Kong J, He X. Urgent transcatheter arterial embolization for Wunderlich syndrome with hypovolemic shock secondary to ruptured renal angiomyolipoma. *Front Surg*. 2021;8:704478. [\[CrossRef\]](#)
 10. Hebert LA, Betts JA, Sedmak DD, Cosio FG, Bay WH, Carlton S. Loin pain-hematuria syndrome associated with thin glomerular basement membrane disease and hemorrhage into renal tubules. *Kidney Int*. 1996;49(1):168-173. [\[CrossRef\]](#)
 11. Antonescu O, Duhamel M, Di Giacinto B, Spain J. Spontaneous renal hemorrhage: a case report and clinical protocol. *Cureus*. 2021;13(6):e15547. [\[CrossRef\]](#)
 12. Naik U, Amin SE, Gehris BT, Wang W, Hunter RL. Papillary renal cell carcinoma with massive hemorrhage: An autopsy case report. *Am J Clin Pathol*. 2022;158(Suppl 1):32. [\[CrossRef\]](#)
 13. Lu J, Zhou W, Wei X, Wang K, Zhou L, Xu X. Clear cell renal cell carcinoma metastasized to the ampulla of Vater 16 years after nephrectomy—a rare case. *Diagnostics (Basel)*. 2022;12(3):571. [\[CrossRef\]](#)
 14. Turner NN, Turner NN, Lameire N, et al. eds. *Oxford Textbook of Clinical Nephrology*. Oxford University Press; 2015. [\[CrossRef\]](#)
 15. Johnstone C, Rich SE. Bleeding in cancer patients and its treatment: a review. *Ann Palliat Med*. 2018;7(2):265-273. [\[CrossRef\]](#)
 16. Swensen SJ, McLeod RA, Stephens DH. CT of extracranial hemorrhage and hematomas. *Am J Roentgenol*. 1984;143(4):907-912. [\[CrossRef\]](#)
 17. Kawashima A, Sandler CM, Ernst RD, et al. Imaging of nontraumatic hemorrhage of the adrenal gland. *Radiographics*. 1999;19(4):949-963. [\[CrossRef\]](#)
 18. Caskey CI. Ultrasound techniques for evaluating renal masses, renal obstruction, and other upper tract pathology. *Ultrasound Q*. 2000;16(1):23-39. [\[CrossRef\]](#)
 19. Semelka RC. *Abdominal-Pelvic MRI*. Fourth. 2016. [\[CrossRef\]](#)
 20. Ren JH, Ma N, Wang SY, et al. Rationale and study design for one-stop assessment of renal artery stenosis and renal microvascular perfusion with contrast-enhanced ultrasound for patients with suspected renovascular hypertension. *Chin Med J (Engl)*. 2019;132(1):63-68. [\[CrossRef\]](#)
 21. Çıldıg MB, Gök M, Abdullayev O. Pre-procedural shear wave elastography on prediction of hemorrhage after percutaneous real-time ultrasound-guided renal biopsy. *Radiol Med*. 2020;125(8):784-789. [\[CrossRef\]](#)
 22. Gomella PT, Telfer S, Lebatschi A, et al. MP42-15 Timing, incidence and management of delayed bleeding after partial nephrectomy in patients at risk for recurrent, bilateral, multifocal renal tumors. *J Urol*. 2024;201(Suppl 4):e613. [\[CrossRef\]](#)
 23. Al Awwad A, Alshubaili H, Mohamed AY, Abuanz S. Incidental finding of bilateral ovarian and renal veins thromboses post cesarean hysterectomy complicated by ureteric injury: First case presentation. *Urol Ann*. 2022;14(3):288-291. [\[CrossRef\]](#)
 24. Kato T, Masui K, Yoshida T, et al. Acquired hemophilia A developing at bilateral renal bleeding: a case report. *Hinyokika Kyo*. 2009;55(4):215-218. [\[CrossRef\]](#)
 25. Tsurusaki T, Maruta N, Iwasaki S, Saito Y. Acquired haemophilia A presenting as acute renal failure secondary to bilateral renal bleeding. *BJU Int*. 2002;90(4):40-41. [\[CrossRef\]](#)
 26. Chang JM, Moon WK, Cho N, et al. Clinical application of shear wave elastography (SWE) in the diagnosis of benign and malignant breast diseases. *Breast Cancer Res Treat*. 2011;129(1):89-97. [\[CrossRef\]](#)
 27. Moschouris H, Papadaki MG, Spanomanolis N, Stamatiou K, Malagari K. Percutaneous thrombin injection under contrast-enhanced ultrasound guidance to control active extravasation not associated with pseudoaneurysm. *Diagn Interv Radiol*. 2023;29(4):632-637. [\[CrossRef\]](#)
 28. Massimo T, Emanuela P. Iatrogenic renal pseudoaneurysm following laparoscopic tumorectomy: CT diagnosis and interventional treatment. [\[CrossRef\]](#)
 29. Haacke EM, Mittal S, Wu Z, Neelavalli J, Cheng YC. Susceptibility-weighted imaging: technical aspects and clinical applications, part 1. *AJNR Am J Neuroradiol*. 2009;30(1):19-30. [\[CrossRef\]](#)
 30. Beauchamp MH, Ditchfield M, Babl FE, et al. Detecting traumatic brain lesions in children: CT versus MRI versus susceptibility weighted imaging (SWI). *J Neurotrauma*. 2011;28(6):915-927. [\[CrossRef\]](#)
 31. Sehgal V, Delproposto Z, Haacke EM, et al. Clinical applications of neuroimaging with susceptibility-weighted imaging. *J Magn Reson Imaging*. 2005;22(4):439-450. [\[CrossRef\]](#)
 32. Haacke EM, Xu Y, Cheng YCN, Reichenbach JR. Susceptibility weighted imaging (SWI). *Magn Reson Med*. 2004;52:612-618. [\[CrossRef\]](#)
 33. Roubidoux MA. MR imaging of hemorrhage and iron deposition in the kidney. *Radiographics*. 1994;14(5):1033-1044. [\[CrossRef\]](#)
 34. Xing W, He X, Kassir MA, et al. Evaluating hemorrhage in renal cell carcinoma using susceptibility weighted imaging. *PLoS One*. 2013;8(2):e57691. [\[CrossRef\]](#)
 35. Li D, Pua BB, Madoff DC. Role of embolization in the treatment of renal masses. *Semin Intervent Radiol*. 2014;31(1):70-81. [\[CrossRef\]](#)
 36. Zhang JQ, Fielding JR, Zou KH. Etiology of spontaneous perirenal hemorrhage: a meta-analysis. *J Urol*. 2002;167(4):1593-1596. [\[CrossRef\]](#)
 37. Newatia A, Khatri G, Friedman B, Hines J. Subtraction imaging: applications for nonvascular abdominal MRI. *AJR Am J Roentgenol*. 2007;188(4):1018-1025. [\[CrossRef\]](#)
 38. Morris CS, Baerlocher MO, Dariushnia SR, et al. Society of interventional radiology position statement on the role of percutaneous ablation in renal cell carcinoma: endorsed by the Canadian Association for Interventional Radiology and the Society of Interventional Oncology. *J Vasc Interv Radiol*. 2020;31(2):189-194. [\[CrossRef\]](#)
 39. McDougal WS, Kursh ED, Persky L. Spontaneous rupture of the kidney with perirenal hematoma. *J Urol*. 1975;114(2):181-184. [\[CrossRef\]](#)
 40. Prasad SR, Sahani DV, Mino-Kenudson M, et al. Neoplasms of the perivascular epithelioid cell involving the abdomen and the pelvis: cross-sectional imaging findings. *J Comput Assist Tomogr*. 2007;31(5):688-696. [\[CrossRef\]](#)
 41. Katabathina VS, Vikram R, Nagar AM, Tamboli P, Menias CO, Prasad SR. Mesenchymal neoplasms of the kidney in adults: imaging spectrum with radiologic-pathologic correlation. *Radiographics*. 2010;30(6):1525-1540. [\[CrossRef\]](#)
 42. Moratalla MB. Wunderlich's syndrome due to spontaneous rupture of large bilateral angiomyolipomas. *Emerg Med J*. 2009;26(1):72. [\[CrossRef\]](#)

43. Nabi N, Shaikh AH, Khalid SE. Tuberos sclerotic with bilateral renal angiomyolipoma and Wunderlich's syndrome. *J Coll Physicians Surg Pak*. 2007;17(11):706-707. [\[CrossRef\]](#)
44. Arrabal-Polo MA, Arrabal-Martin M, Palao-Yago F, et al. Wunderlich syndrome from a malignant epithelioid angiomyolipoma. *Urol J*. 2009;6(1):50-53. [\[CrossRef\]](#)
45. Sherman JL, Hartman DS, Friedman AC, Madewell JE, Davis CJ, Goldman SM. Angiomyolipoma: computed tomographic-pathologic correlation of 17 cases. *Am J Roentgenol*. 1981;137(6):1221-1226. [\[CrossRef\]](#)
46. Eble JN. Angiomyolipoma of kidney. *Semin Diagn Pathol*. 1998;15(1):21-40. [\[CrossRef\]](#)
47. Yamakado K, Tanaka N, Nakagawa T, Kobayashi S, Yanagawa M, Takeda K. Renal angiomyolipoma: Relationships between tumor size, aneurysm formation, and rupture. *Radiology*. 2002;225(1):78-82. [\[CrossRef\]](#)
48. Woo S, Kim SY, Cho JY, Kim SH, Lee MS. Exophytic renal angiomyolipoma and perirenal liposarcoma: revisiting the role of CT for differential diagnosis. *Acta Radiol*. 2016;57(2):249-255. [\[CrossRef\]](#)
49. Kış N, Düzkalır HG, Ağaçlı MO, Erok B, Kılıçoğlu ZG. Contribution of diffusion weighted MRI to the differential diagnosis of renal masses. *Eur J Clin Exp Med*. 2022;20(1):44-48. [\[CrossRef\]](#)
50. Wang C, Yang M, Tong X, et al. Transarterial embolization for renal angiomyolipomas: a single centre experience in 79 patients. *J Int Med Res*. 2017;45(2):706-713. [\[CrossRef\]](#)
51. Planché O, Correas JM, Mader B, Joly D, Méjean A, Hélénon O. Prophylactic embolization of renal angiomyolipomas: evaluation of therapeutic response using CT 3D volume calculation and density histograms. *J Vasc Interv Radiol*. 2011;22(10):1388-1395. [\[CrossRef\]](#)
52. Hongyo H, Higashihara H, Osuga K, et al. Efficacy of prophylactic selective arterial embolization for renal angiomyolipomas: identifying predictors of 50% volume reduction. *CVIR Endovasc*. 2020;3(1):84. [\[CrossRef\]](#)
53. Faddegon S, So A. Treatment of angiomyolipoma at a tertiary care centre: the decision between surgery and angioembolization. *Can Urol Assoc J*. 2011;5(6):138-141. [\[CrossRef\]](#)
54. Asghar M, Ahmed K, Shah SS, Siddique MK, Dasgupta P, Khan MS. Renal vein thrombosis. *Eur J Vasc Endovasc Surg*. 2007;34(2):217-223. [\[CrossRef\]](#)
55. Ahn T, Roberts MJ, Navaratnam A, Chung E, Wood S. Changing etiology and management patterns for spontaneous renal hemorrhage: a systematic review of contemporary series. *Int Urol Nephrol*. 2017;49(11):1897-1905. [\[CrossRef\]](#)
56. Kawashima A, Sandler CM, Ernst RD, Tamm EP, Goldman SM, Fishman EK. CT evaluation of renovascular disease. *RadioGraphics*. 2000;20(5):1321-1340. [\[CrossRef\]](#)
57. Zapzalka DM, Thompson HA, Borowsky SS, Coleman-Stenson CC, Mahowald ML, O'Connell KJ. Polyarteritis nodosa presenting as spontaneous bilateral perinephric hemorrhage: management with selective arterial embolization. *J Urol*. 2000;164(4):1294-1295. [\[CrossRef\]](#)
58. Stanson AW, Friese JL, Johnson CM, et al. Polyarteritis nodosa: spectrum of angiographic findings. *Radiographics*. 2001;21(1):151-159. [\[CrossRef\]](#)
59. Eldem G, Erdoğan E, Peynircioğlu B, Arat A, Balkancı F. Endovascular treatment of true renal artery aneurysms: a single center experience. *Diagn Interv Radiol*. 2019;25(1):62-70. [\[CrossRef\]](#)
60. Noshier JL, Chung J, Brevetti LS, Graham AM, Siegel RL. Visceral and renal artery aneurysms: a pictorial essay on endovascular therapy. *Radiographics*. 2006;26(6):1687-1704. [\[CrossRef\]](#)
61. Sheth S, Ali S, Fishman E. Imaging of renal lymphoma: patterns of disease with pathologic correlation. *Radiographics*. 2006;26(4):1151-1168. [\[CrossRef\]](#)
62. Heiken JP, Gold RP, Schnur MJ, King DL, Bashist B, Glazer HS. Computed tomography of renal lymphoma with ultrasound correlation. *J Comput Assist Tomogr*. 1983;7(2):245-250. [\[CrossRef\]](#)
63. Urban BA, Fishman EK. Renal lymphoma: CT patterns with emphasis on helical CT. *Radiographics*. 2000;20:197-212. [\[CrossRef\]](#)
64. Chepuri NB, Strouse PJ, Yanik GA. CT of renal lymphoma in children. *Am J Roentgenol*. 2003;180(2):429-431. [\[CrossRef\]](#)
65. Cohan RH, Dunnick NR, Leder RA, Baker ME. Computed tomography of renal lymphoma. *J Comput Assist Tomogr*. 1990;14(6):933-938. [\[CrossRef\]](#)